Technical and Environmental Assessment of the Consequences of Accidents on Offshore Gas Pipelines in the Baltic Sea

Yakov Masyutin[1], Pavel Shcherban[2], Andrey Gusev[3], Anna Vatagina[1]

The failure of the Nord Stream pipelines in the Baltic Sea in September 2022 had significant technical and economic consequences not only for the European Union energy sector and the gas production and transmission industry of the Russian Federation, but also entailed a number of environmental consequences, the scale of which has yet to be explored. During the preliminary assessment of the consequences of the accident, the team of scientists from the Kant Baltic Federal University, the Atlantic branch of the VNIRO and the Shirshov Oceanology Institute of the Russian Academy of Sciences calculated the composition of the gas mixture emitted and assessed its volume, studied potential environmental damage to the biogeocenoses of the Western and Southern Baltic, calculated the impact of the gases emitted on global temperature. The studies were based on data obtained from open sources and allow us to give a preliminary assessment of the environmental impact of the accident. The combination of analytical, evaluation and research methods used is basically a classic approach to accounting for the volume of gas emissions and their subsequent impact. Leakage volume was calculated by first determining the volume of gas that entered the natural environment after impact (before the emergency valves were closed), and then determining the second volume of gas (until pressure stabilization in the cut-off pipe sections and in the environment). Based on the information on the biota in the water area and the nature of the gas movement, an estimated impact on biological organisms in the zone of the Bronholm depression was determined. Based on the models of the influence of methane emissions on climatic parameters, the preliminary consequences of the emission were established. The assessment of the environmental impact on the water area was conducted and the main directions of further research determined. The potential ways to minimize the environmental consequences of the accident in the short and long term have been considered.

KEY WORDS

~ Natural gas release
~ Technogenic accident
~ Baltic Sea
~ Marine ecology
~ Offshore gas pipelines
~ Baltic biogeocenoses

[1] Immanuel Kant Baltic Federal University, Institute of Medicine and Life Sciences, Higher School of Living Systems, Kaliningrad, Russia
[2] Immanuel Kant Baltic Federal University, Institute of High Technology, Higher School of Interdisciplinary Research and Engineering, Kaliningrad, Russia
[3] Russian Academy of Sciences, Shirshov Institute of Oceanology, ATLANTNIRO, Kaliningrad, Russia

e-mail: ursa-maior@yandex.ru

doi: 10.7225/toms.v13.n01.w01
Received: 25 Jul 2023 / Revised: 11 Nov 2023 / Accepted: 19 Nov 2023 / Published: 22 Nov 2023

1. INTRODUCTION

The Nord Stream system pipelines consist of four almost parallel strings (Haynes & Daetwyler, 2012). During pipeline construction in 2010-2012 and 2020-2021, the engineers and builders chose the shortest route between Russia and Germany, avoiding the deepest parts of the Baltic Sea, dumps and weapons storage areas and areas with rugged, rocky ground (Nikitina, 2014). The 2022 accident occurred in the Bornholm Basin in the Baltic Sea, a stable zone with depths ranging from -75 to -100 meters. The accidents occurred on three of the four strings. Nord Stream 1A and B - two accidents (in the northern part of the Bornholm Basin), accident coordinates: 55°33'400" N 015°47'300" E and 55°32'450" N 015°46'470" E. Nord Stream 2A - also two accidents, one in the northern part and another on the border of the western part of the Bornholm Basin, accident coordinates: 55°32'100" N 015°41'900" E and 54°52'600" N 015°24'600" E. In all these instances, approximately 50-75 m of pipes were completely destroyed. At the same time, up until the pumping stoppage system was triggered, gas continued to flow under pressure through the ruptures. After the supply was stopped, there was a gradual release of gas from the pipe sections (between rupture points and the point where either the cut-off valve was triggered, or the gas-water level was equalized by hydrostatic forces).

Thus, the environmental impact of accidents was found to have at least three stages (Environment and Energy, 2013). Firstly, there was the blast wave from each of the emergency points. Second, there was an abrupt release of natural gas. And, third, there was the leakage of natural gas from the cut-off sections of the pipelines. In this study, we simulated the process of release and subsequent leakage of natural gas from each damaged section and calculated preliminary emission volumes. Taking into account the bottom currents in the Bornholm Basin, the directions of natural gas distribution in the water were considered. A preliminary assessment of the impact of accidental emissions on the biotopes of the Bornholm Basin was made.

It should be noted that despite the fact that natural gas, unlike oil, escapes the aquatic environment into air rather quickly, since the examined basin belongs to the areas of the Baltic Sea with low oxygen levels, the impact on biota may be more significant. Of course, preliminary results of gas emission volume and environmental impact assessment will be further clarified by complex research - soil and water sampling, benthos, plankton and nekton sampling.

Several authors have already published research on this issue, i.e. the Nord Stream pipeline explosion in particular and environmental impact of gas pipeline damage in general. The paper by Sanderson H. et al. is dedicated to the impact on the marine ecosystem rather than on climate change (Sanderson, 2023). The authors stressed the negative consequences of gas release on the population of harbor porpoises, seals, and fish. The paper by Kiciński R. addresses the issues of crater size estimation after an underwater “Nord Stream” explosion (Kiciński, 2023). The author concluded that the data obtained from Danish researches suggest that the explosives were equivalent to 500-750 kg of TNT, as 750 kg of TNT create the crater having the volume of approx. 20 m^3. The environmental impact of gas bubbles and pressure wave pulses on marine fauna was found to be significant. The paper by H. Lu et al. is dedicated to natural gas pipeline incidents in the USA and Canada from 1980s to 2021 (Lu et al., 2023). Despite being considered the critical transitional source of energy, damaged natural gas pipelines emit a huge quantity of greenhouse gases (GHG), such as methane and carbon dioxide from flares gas, into the atmosphere. The authors wanted to include these significant emissions in the regular system of GHG emissions inventory.

The true reasons behind this environmental disaster are still a matter of conjecture. Of course, it was a thoroughly planned operation involving conspiracy. To the present day, most researches are in a quandary, and nobody can give a definite answer who was behind this incident (Yin & Zhong, 2023).

2. TECHNICAL CONSEQUENCES OF THE ACCIDENT. CALCULATION OF THE VOLUME OF GAS LEAKAGE FROM THE NORTH STREAM PIPELINES INTO THE ENVIRONMENT

Research methodology consists of three interconnected parts. The first stage involved the direct calculation of gas leakage volume based on all available open data. In the second stage, the impact of gas leakage volume on local biogeocenoses, benthos, nekton and plankton, was assessed, while the impact of the volume of gas emissions on the global ecosystem was determined in the third stage (by assessing atmospheric temperature increase).

While calculating results for natural gas leakage from the Nord Stream system pipelines, the widest range of factors was taken into account, including: factors and parameters of the natural environment, factors and parameters of the pipeline system, technological features of the pumping process, etc. It should be noted that in a number of cases we had to use averaged or approximate data when modeling processes and calculating natural gas leakage volumes (due to the lack of publicly available information at the time of the study). Nevertheless, the results give a general idea on the nature of the emergency situation and environmental consequences to be determined in subsequent studies.

The main parameters of the pipeline system used in the analytical model are as follows: pipeline diameter (1200 mm); gas pressure in the system at breakdown points (about 190 bar) (Tichý & Dubský, 2020); composition of the transported gas mixture (methane 95%, ethane 3%, nitrogen 1%, other gases - 1%), length of the damaged section (due to preliminary data we accepted the length of 50 m), duration of the gas leak (depending on point, speed of valve system actuation, gas pumping stop, hydrostatic pressure equalization from 1 to 4 hours), temperature of transported gas - (about 10^{o}C).

The main natural environment parameters considered (depending on accident location) are: the depth of occurrence of the accidental release of natural gas (from -74 to -85 m), current speed on the bottom and in the water mass of the Bornholm basin (2-2.5 cm per second) (Stigebrandt et al., 2015), flow direction, the concentration of oxygen (0-10 ml/l) and hydrogen sulfide compounds (0-2 ml/l) in the water mass, sea salinity in the area observed (from 7 psu at the surface to 22 psu at the bottom) (Kuliński et al., 2022), as well as other parameters (fig. 1).

Technological characteristics of the pumping process, the availability of gas shut-off system in the pipeline, with shut-off valves installed every 15-18 km, as well as the rate of shutting off the pipelines and stopping the gas pumping (Tichý & Dubský, 2020) were taken into account. The process of natural gas release proceeded in several stages. The greatest quantity of gas was released immediately after pipeline rupture, followed by the steady release of gas from the ruptured pipeline under pumping pressure, and once the pumping stopped, the remaining gas kept leaking until the hydrostatic level was stabilized over the system elements (Jin et al., 2014).

The calculation of the volume of natural gas release for each of the gas pipeline sections was carried out by calculating and summing up the volume released at the moment of the accident, until pumping stopped, and until the hydrostatic level equalized (or until shutoff mechanism triggering) (Shcherban & Mazur, 2023).

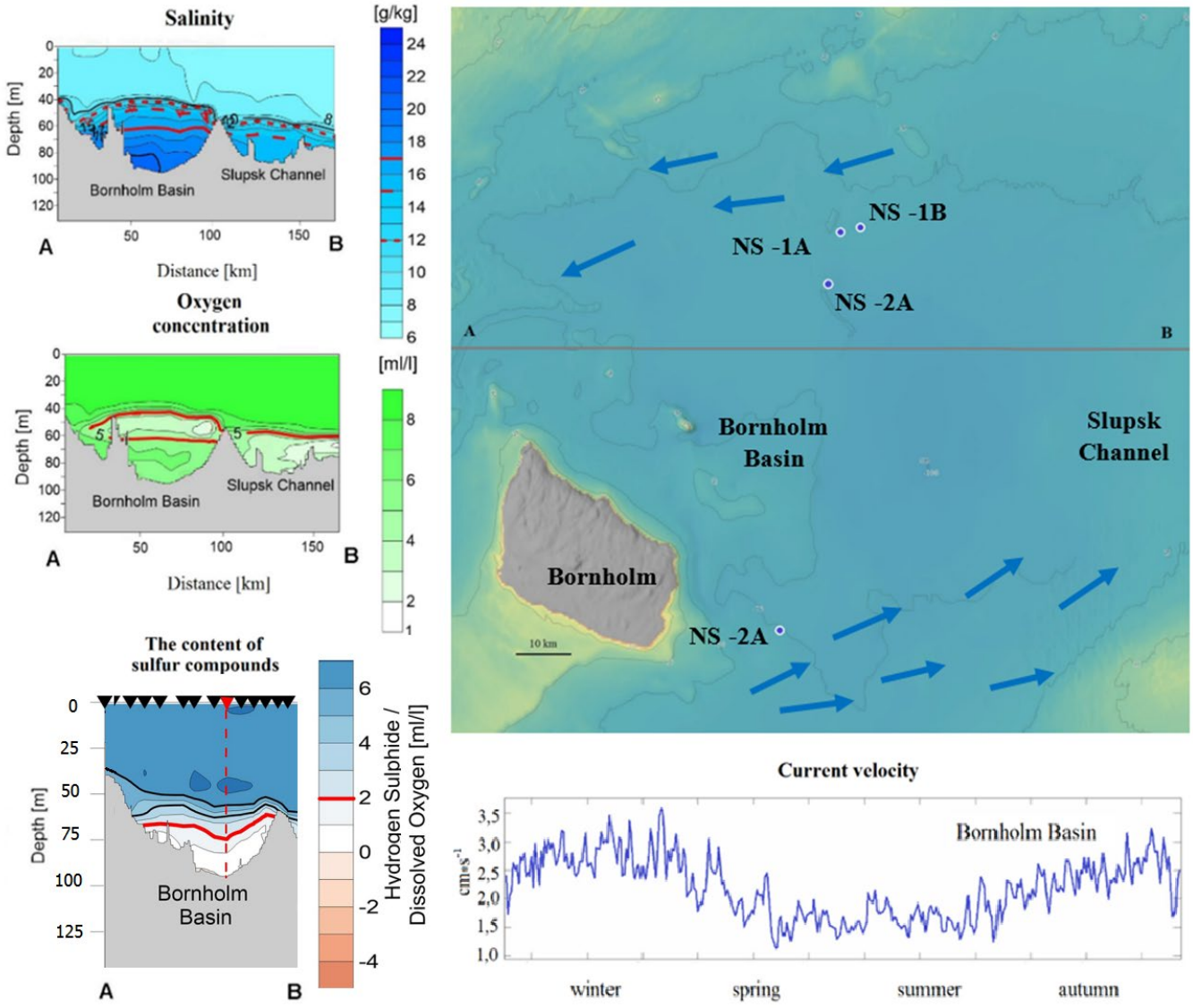

Figure 1. The Bornholm Basin. Natural gas leakage points and natural characteristics of the aquatic environment. Based on (Stigebrandt et al., 2015; Kuliński et al., 2022).

Therefore, a system of differential equations of one-dimensional unsteady and nonisothermal gas flow in the gas pipeline was used (Lurie et al., 2020):

$$\begin{cases} \frac{\partial p}{\partial t} + \frac{\partial pv}{\partial x} = 0; \\ \frac{\partial pv}{\partial t} + \frac{\partial}{\partial x}(\mathrm{P} + pv^2) = -\lambda(Re_i\varepsilon)\frac{1}{d_0}\cdot\frac{pv^2}{2} - pg\sin\alpha; \\ p\left(\frac{\partial e^{int}}{\partial t} + v\frac{\partial e^{int}}{\partial x}\right) = \frac{4k}{d_0}(T - T_n) - \mathrm{P}\frac{\partial v}{\partial X} + \lambda(Re_i\varepsilon)\frac{1}{d_0}\cdot\frac{pv^3}{2}; \end{cases} \quad (1)$$

Where: $p(x,t)$ - gas density; $v(x,t)$ - gas velocity; P - gas pressure; $T(x,t)$ - absolute gas temperature; T_n- outdoor temperature; k- heat transfer coefficient; $e^{int}(T) = C_vT + const$ - internal energy of gas; C_v - heat capacity of gas at constant volume; $p = \frac{\mathrm{P}}{\mathrm{ZRT}}$ - gas equation; $Z(\mathrm{P},T)$ - gas supercompressibility coefficient at the depth of break points in the sea; $\lambda(Re_i\varepsilon)$ - hydraulic resistance coefficient; d_0 - pipeline diameter; $Re = vd_0/v$ - Reynolds number; v – kinematic viscosity of the gas; ε - relative roughness of the inner surface of the gas pipeline; α – angle of the pipeline axis to the horizon; g – gravitational acceleration. The unknowns are functions $\mathrm{P}(x,t)$ and $T(x,t)$, which depend on the coordinate x and time t.

It should be noted that the resulting system of differential equations can be solved by a sequential transition from the equation of internal energy of gas to enthalpy - $J\,(p,T) = e^{int} + \text{P}/p$. The second equation is then multiplied by gas velocity and the product of the third equation subtracted, obtaining a system of partial differential equations used to determine three unknown functions $\text{P}(x,t)$, $T(x,t)$ and $v(x,t)$, dependent on coordinate x and time t (Bezrodny et al., 2020).

$$\begin{cases} \left(\frac{\partial \text{P}}{\partial p}\right)_T \frac{\partial p}{\partial t}\left(\frac{\partial p}{\partial T}\right)_p \frac{\partial T}{\partial t} + v\left(\frac{\partial p}{\partial p}\right)_T \frac{\partial p}{\partial x} + v\left(\frac{\partial p}{\partial T}\right)_p \frac{\partial T}{\partial x} + p\frac{\partial v}{\partial x} = 0; \\ \text{P}\frac{\partial v}{\partial t} + \text{P}v\frac{\partial v}{\partial x} + \frac{\partial p}{\partial x} = J_2; \\ \text{P}C_p\frac{\partial T}{\partial t} + \text{P}vC_p\frac{\partial T}{\partial x} - \left(\text{P}C_pD + 1\right)\frac{\partial \text{P}}{\partial t} - \left(\text{P}C_pD + 1\right)v\frac{\partial p}{\partial x} = J_3 \\ \text{P} = p/(ZRT); \end{cases} \quad (2)$$

Where: $J_2 = -\frac{\lambda \text{P}v|v|}{2d} - pg \cdot dz/dx$; $J_3 = -\frac{4K_T\left(T - T_{\text{нар}}\right)}{d + \lambda \text{P}v^3/2d}$

The obtained nonlinear system is difficult to solve. However, it is worth mentioning that there are two special lines (characteristics), $x = \pm c$, for poorly compressible fluids or gases on the plane of variables, along which the system of partial differential equations transforms into the ordinary differential equation for a certain combination of required functions (Lurie, 2008). Likewise, being a system of equations with two unknowns with exactly two characteristics, it belongs to the class of hyperbolic systems, allowing the use of a method of characteristics for its solution. It is beyond the scope of this study to outline the principles of the method of characteristics. It is presented in detail in the works of, e.g. Lurie, M. V., Pulch, R., and Günther, M.

When this method is applied and time derivatives replaced with finite-difference analogues in the final stage, a system of algebraic equations is obtained which can be used to determine each of the required values (Zavyalov et al., 2023). In this case, gas leak volume value needs to be determined first.

$$\begin{cases} \text{P}_m = \frac{(\text{pc})_{\text{в}} \cdot \Phi_{\text{A}} + (\text{pc})_{\text{A}} \Psi_B}{(\text{pc})_A + (\text{pc})_{\text{в}}}; \\ \text{V}_m = \frac{\Phi_{\text{A}} - \Psi_B}{(\text{pc})_A + (\text{pc})_{\text{в}}}; \\ T_m = \Theta_c + \left\{\frac{1}{pC_p}\left[1 + \frac{T}{Z}\left(\frac{\partial Z}{\partial T}\right)_p\right]\right\}_c \cdot \text{P}_m \end{cases} \quad (3)$$

The aforementioned lower letter indices m – refer to the calculation for a particular point (Pulch & Günther, 2022). Please note that the pipeline destruction occurred over a large area. But to simplify, every segment of pipeline rupture was considered a point in this study (Lurie, 2009). Therefore, the calculation process involved determining gas volumes at eight points and at different modes (short-term mode of pressure flow until valve closing and long-term modes of unsteady gas flow until pressure equalization with the environment). During the calculations, initial and boundary, as well as coupling conditions, were added to the main system equations, modeling the work of shut-off valves located on the gas pipeline (Leighton & White, 2012). Initial conditions represent initial pipeline state, i.e. the state of the pipeline prior to gas leakage. Boundary conditions at the ends of the observed pipeline section reflect the processes of interaction of that respective section with the rest of the pipeline. Either gas pressure on the right end of the section through which gas is flowing (a working gas source, such as a compressor station) was set at a particular value or gas flow rate was set to 0 (once gas source was disconnected).

In the right part of the section through which the gas is withdrawn, either gas pressure was set at a particular value (until the gas flow rate is reduced to the value set by the "protection setting") or gas flow rate was set to 0 (Li et al., 2022). Gas leakage volume results for each of the Nord Stream subsea pipeline strings are summarized in Table 1, which also shows the resulting total (methane) emission volume over the entire time.

Were an accident to occur at valve location (worst case scenario), “shut-off valves need to be installed on the linear part of the pipelines, at calculated distance not greater than 30 km.” (SNiP 2.05.06 - 85*). X_1 and x_2 are the distances from the breaking point to the next locking device.

Pipeline string	NS-1A		NS-1B		NS-2A	
	x_1	x_2	x_1	x_2	x_1	x_2
estimated distance between point of accident and line valve (km)	30	30	30	30	30	30
mass of gas over the entire period of leakage from breaking point (tons)	18 217,8		17 851,08		44 246,12	
mass of gas over the entire leakage period (in megatons)	0,0803					

Table 1. The results of calculation of methane emissions from the Nord Stream-1 and 2 gas pipelines.

As previously indicated, pipeline-water gas leakage consists of three stages: flow creation (or reactive zone), jet flow, hydrostatic pressure equalization in the pipeline system, and methane flow-water interaction. Gas movement in the flow creation zone is characterized by high velocity and turbulence. Gas movement in this zone is characterized by the high initial momentum of the flowing gas (Leighton & White, 2012). On its way to the sea surface, the gas expands and forms a bubble. On the one hand, the breaking force of surrounding water acts on the gas bubble; on the other hand, the gas transmits its momentum to the environment. The interaction between gas and water causes the liquid fragment entrainment phenomenon (Li et al., 2022). In the clean jet zone, the value of gas momentum is low. Archimedes' force is the dominant driving force, causing the gas to rise to the surface. In this zone, the size of the bubbles depends on turbulence parameters.

As the gas approaches sea surface, the water drops near the interfacial boundary spread in the radial direction of the horizontal surface, carrying the gas bubbles with them. When the gas bubble reaches sea surface, a fountain forms in the interaction zone (Leighton & White, 2012). Many bubbles break the surface making their way into the atmosphere, causing a boiling zone on the water surface. The "cloud" of dissolved gas moves along the current, extending into a long and narrow strip. The current from "NS-1" moves in the direction of the Danish straits, and the current from "NS-2" to the east of the Baltic Sea. This gas will gradually escape into the atmosphere. On the basis of the analytical data obtained, we generated enlarged models of emissions by leakage points (an example of the model is given in Fig. 2).

A comparison of the calculated data with other analytical and instrumental studies dealing with this issue is interesting. For example, the analytical study conducted by Stéphane Orjollet estimates the leakage volume across all pipeline sections to be approx. 0.07. Forsetlund Solbakken also estimated the leakage volume of gas over the entire period to be between 0.056 and 0.155 megatons (Chen & Zhou, 2023). Instrumental observations from GHGSat are also important (McKeever et al., 2019).

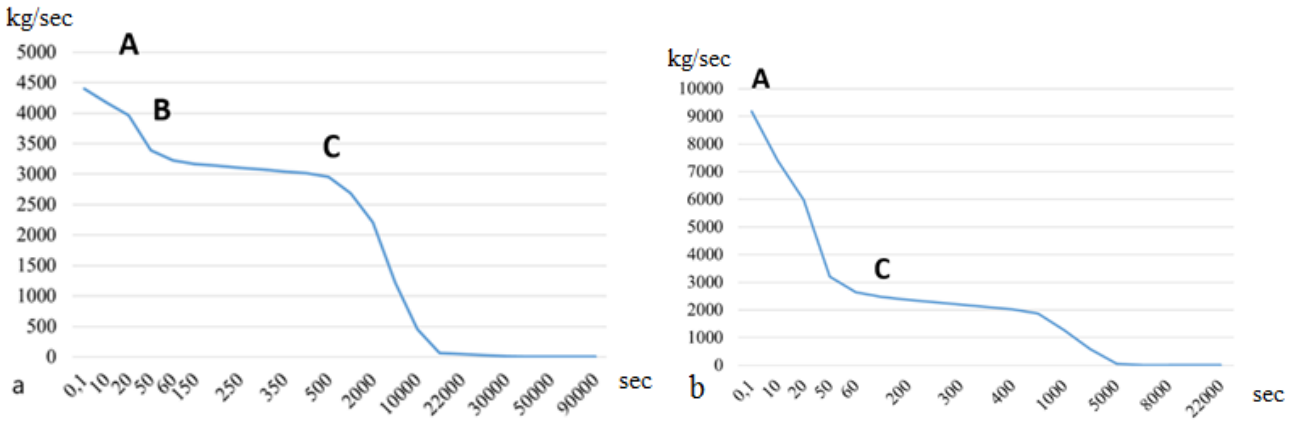

Figure 2. Example of gas emission modeling during a pipeline accident in the Baltic Sea (Nord Stream 1A). a - section of the pipeline from the gas pumping station in Russia to rupture site; b - section from the rupture site to Greifswald. Based on authors' data. A - flow creation stage (leakage flow); B - flow under pressure; C - attenuation stage

GHGSat, the leader in methane emission monitoring from space integral to ESA's third-party mission program, commissioned its satellites to measure gas leakage from the Nord Stream 2 pipeline through a constellation of high resolution satellites (about 25 meters) (fig. 3).

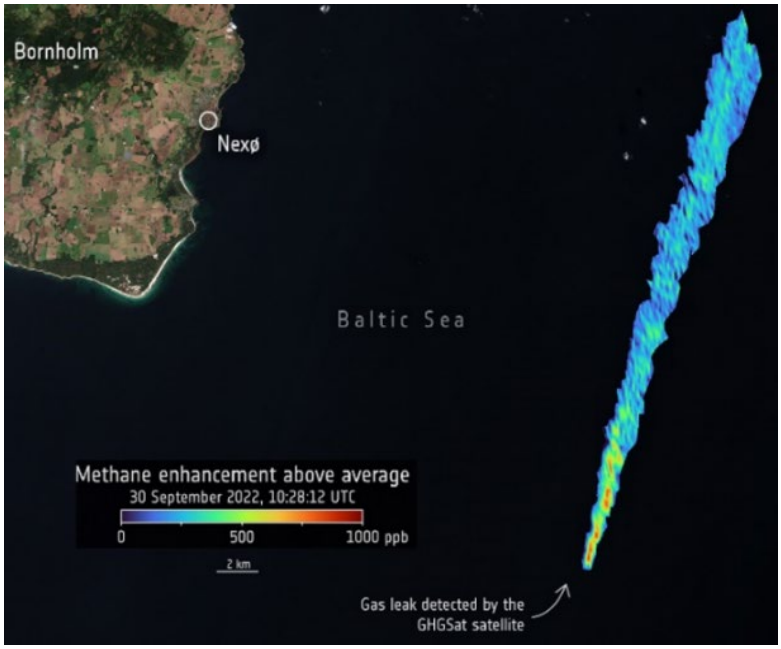

Figure 3. Satellite methane emission sensing results for the Baltic Sea area (Nord Stream-2A). Based on GHGSat data.

The emission rate measured at the first methane measurement, made on September 30, was 79,000 kg per hour, which makes it the largest methane leak ever detected by GHGSat from a single point source. This figure is extremely high, especially considering that four days have passed since the initial rupture, and this is only one of four rupture points in the pipeline. Thus, leakage volume on the fourth day was 21.9 kg/sec. The analytical calculation made by the authors, shows that during the accident on three strings of the Nord Stream pipelines approximately 0.0803 megatons of methane were released into the atmosphere. Preliminary modeling indicates that the leakage of gas from the accident sites continued for up to 6 days.

Comparing the data obtained from different sources, we can say that in general they correlate with each other, despite the differences in the approaches used to calculate leakage volumes. Comparing the data obtained from different sources, we can say that in general they correlate with each other, despite the differences in the approaches used to calculate leakage volumes. Based on the calculations made by the authors, as well as on the data of periodicals and the results of instrumental observations, we can state that the total volume of emission did not exceed 0.100 megatons. Further assessment of the impact of natural gas emissions on the biota of this water area and on the greenhouse effect will be made on the basis of this assumption.

3. TECHNICAL CONSEQUENCES OF THE ACCIDENT. CALCULATION OF THE VOLUME OF GAS LEAKAGE FROM NORTH STREAM PIPELINES INTO THE ENVIRONMENT

Speaking of the biogeocenosis of the Bornholm Basin which was affected by gas emission, let's take a look at the main representatives of its flora and fauna.

During the year the concentration of chlorophyll a in the area of the Bornholm Basin varies from 0.92 to 5.20 mg/m^3. The lowest values are observed in the winter and summer months, and maximums in spring and autumn when phytoplankton blooms. Phytoplankton biomass varies throughout the year from 0.1 to 1.6 g/m^3.

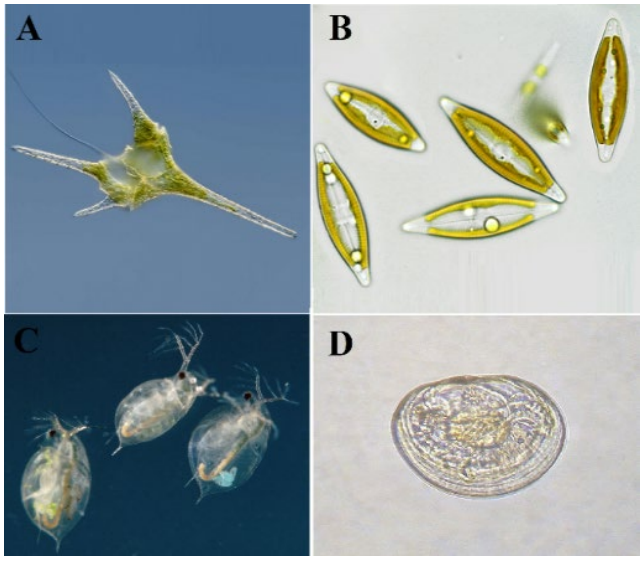

Figure 4. Species of phyto- and zooplankton in the water area studied: A - phytoplankton belonging to the *Dinophyta* division; B - phytoplankton belonging to the *Bacillariophyta* division; C - *Daphnia* belonging to the *Cladocera* division; D - larvae belonging to the *Bivalvia* division.

The spring bloom maximum (usually in May) can be attributed to *Dinophytas*, while *Bacillariophyta* account for the autumn maximum (usually in November) (Dutz et al., 2022; Wasmund at al., 2019; Zettler, 2020). The zooplankton in the Bornholm Basin consists of 13 holoplankton species (*Rotifera*, *Cladocera*, *Copepoda* and *Tunicata*) (fig. 4). The meroplankton contains larvae of *Bivalvia*, *Polychaeta*, *Gastropoda Cirripedia*, *Decapoda* and fish eggs. Zooplankton numbers have significant seasonal fluctuations.

The minimum zooplankton values of approx. 4 thousand sp./m^3 are observed in winter, while the maximum values of 30-40 thousand sp./m^3 and in some months occasionally up to 105 thousand sp./m^3 (Polunina et al., 2021; Schulz et al., 2012) are observed in the summer months. The biomass of zooplankton in August-September is, on average, 0.47 g/m^3 (Polunina et al., 2021). The zoobenthos of the Bornholm Basin has been

poorly studied since the early 2000s (Gogina et al., 2016). However, hypoxia (less than 2 ml O_2/l), which has a significant negative effect on zoobenthos (Karlson et al., 2002; Rolff et al., 2022), has been observed throughout the area. The benthic "desert" zone, where zoobenthos is not present, begins at the depth of 61 m (Gusev & Rudinskaya, 2007). Along the periphery of the benthic "desert" there is a poor, in qualitative and quantitative terms, community of the nectobenthic polychaete *Bylgides sarsi* (Kinberg in Malmgren, 1866) (fig. 5). On average, two zoobenthos species per station have been detected; biomass is 34 specimens/m^2 and 1.0 g/m^2 (Gogina et al., 2016).

Figure 5. A representative of the zoobenthos found in the periphery of the water area studied - *Bylgides sarsi*

The ichthyofauna of the Bornholm Basin includes approximately 30 fish species (Zenkevich, 1963). The most important commercial species are cod *Gadus morhua* (Linnaeus, 1758), Baltic herring *Clupea harengus* (Linnaeus, 1758), sprat *Sprattus sprattus* (Linnaeus, 1758), river flounder *Platichthys flesus* (Linnaeus, 1758) and sea flounder *Pleuronectes platessa* (Linnaeus, 1758). The fishing of Baltic herring and sprat by pelagic fishing gear is of great value here. The use of bottom trawls and fishing of demersal fish species (cod, flounder) is less significant (ICES, 2021), including due to the chemical weapons buried at the bottom of the basin (Paka & Nabatov2022). The Bornholm Basin area is an important spawning area for fish with pelagic eggs (Karaseva et al., 2012; Hinrichsen et al., 2007). The most common marine mammals here are harbor seal (*Phoca vitulina* Linnaeus, 1758), ringed seal (*Pusa hispida* (Schreber, 1775)), grey seal (*Halichoerus grypus* (Fabricius, 1791)) and harbor porpoise (*Phocoena phocoena* (Linnaeus, 1758)) (fig. 6). All these species are listed in the Red Book of the Baltic Sea and are protected (HELCOM, 2013).

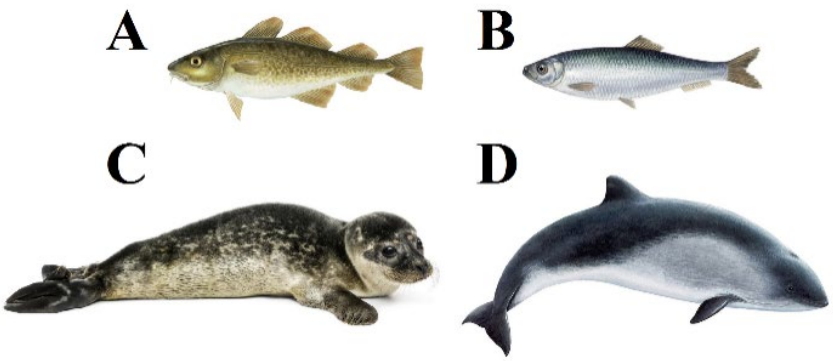

Figure 6. Ichthyofauna and marine mammals in the water area studied: A - cod (*Gadus morhua*); B - sprat (*Sprattus sprattus*); C - harbor seal (*Phoca vitulina*); D - harbor porpoise (*Phocoena phocoena*).

The consequences of the accident on the biogeocenosis are as follows:

- mechanical impact on the bottom, which will result in the death of seabed organisms;
- blow wave - a type of impact causing the redeposition of bottom sediments, as a result of which low-mobile forms of benthos are covered with soil, and die. Planktonic and nektonic animals die as a result of its direct impact or leave the hazardous area;
- increased turbidity and suspended solids in the water, which have a negative effect on animals as they clog their filtration apparatuses, causing their death;

- toxic exposure to pipeline gases escaping to the surface can kill organisms;
- the hydrogen sulfide entrained from the basin also has a devastating effect on living organisms.

Based on the information above, the accident had the lowest impact on benthic communities due to occurring in the area where zoobenthos is either absent or its population density is extremely low. The most significant impact seems to be on phytoplankton, zooplankton and ichthyoplankton communities, which are not capable of active long-term movements. Ichthyofauna and aquatic mammals most likely left the accident area. Thus, based on the speed of the emergency situation, the specifics of the area, the type of gas release and its chemical characteristics, the direct environmental damage to the local fauna and flora of the water area seems to be insignificant. Detailed results are to be obtained after the collection and processing of materials based on the results of the expeditions. Gas emission may have a greater impact on the biosphere in general, since the methane released into the atmosphere and introduced into the carbon cycle has a strong greenhouse effect.

4. AN ASSESSMENT OF THE POTENTIAL IMPACT OF NATURAL GAS EMISSIONS FROM THE NORD STREAM PIPELINES ON THE RATE OF GLOBAL WARMING

In order to analyze the potential impact of natural gas emissions from Nord Stream 1 and Nord Stream 2 pipelines on the rate of global warming and the greenhouse effect progression, the main indicators of the impact of methane have been calculated. Emission volumes can be calculated for each component based on the calculated leakage volumes and quality requirements for transported natural gas (Table 2).

Gas type	Estimated emission volume, Mt
CH_4	0,0803
C_2H_6	0,0025
C_{3+}	0,0008
The sum of hydrocarbons	0,0833
CO_2	0,0002
TOTAL	0,0835

Table 2. Results of greenhouse gas emission volume calculations after the Nord Stream 1 and Nord Stream 2 pipeline accidents

Next, a number of indicators that determine the degree of emission impact on temperature changes were calculated. Temperature fluctuations attributable to a number of natural processes have been a normal occurrence in the Earth's history. Moreover, most greenhouse gases are recycled over time by biota, owing to the presence of natural safety mechanisms in the biosphere (this period is approximately 20 years for methane). The results obtained will show the impact of leaks on temperature changes, which is reversible.

Absolute Global Warming Potential (*AGWP*) is the total radiative forcing produced by a one-kg emission of a given substance into the atmosphere at the beginning of the time horizon:

$$AGWP_i(H) = \int_0^H RF_i\,(t)dt = A_i\tau(1 - \exp\left(-\frac{H}{\tau}\right)) \qquad (4)$$
$$RF_i = A_i \cdot R_i$$

where t – is the time elapsed after the emission; τ – is the lifetime of a greenhouse gas in years; H – is the time horizon in years; RF_i – is the radiative forcing due to pulse gas emission i; A_i – is the radiative forcing of RF_i per unit of the mass increase of i-gases in the atmosphere («radiative efficiency » (RE) W m^{-2} kg^{-1}); R_i – is the

fraction of i-gases remaining in the atmosphere after pulse emissions over time *t* (Intergovernmental Panel on Climate Change 2013, 2014).

The lifetime of CO_2 in the atmosphere is between 300 and 1,000 years, while the absolute global warming potential of carbon dioxide is more complex:

$$AGWP_i(H) = A_{CO_2}\left\{a_0 H + \sum_{i=1}^{l} a_i\,\tau_i\left(1 - \exp\left(-\frac{H}{\tau_i}\right)\right)\right\} \qquad (5)$$

The CO_2 response function is based on the revised version of the Bern model of the carbon cycle used in Chapter 10 of the report (Strassmann & Joos, 2017), where the base value of CO_2 concentration = 378 ppm is applied. The attenuation of the CO_2 pulse over time t is expressed by the following formula:

$$a_0 + \sum_{i=1}^{3} a_i \cdot e^{-t/\tau} \qquad (6)$$

where a_0 = 0,217; a_1 = 0,259; a_2 = 0,338; a_3 = 0,186; τ_1 = 172,9 years; τ_2 = 18,51 years; τ_3 = 1,186 years.

According to this definition, the absolute global warming potential of a given substance depends on its radiative efficiency and removal rate from the atmosphere (in the case of first-order kinetics, it depends on the lifetime in the atmosphere) (Lifshits et al., 2018).

The global warming potential (*GWP*) and time horizon of a substance are defined as the ratio of values of the absolute global warming potential of the substance *AGWP* and a reference substance $AGWP_r$:

$$GWP = \frac{AGWP}{AGWP_r} \qquad (7)$$

Thus, for the reference substance *GWP* is equal to 1 at any choice of time horizon for exposure estimation. CO_2 is taken as a reference substance. *GWP* is a dimensionless value (Lifshits et al., 2018; Gillett & Matthews, 2010).

Based on the above formulas, the global warming potential of methane and carbon dioxide for gas leakage volumes from gas pipelines (table 3, fig. 7) was calculated, taking into account the fact that uncertainties in the determination of *GWP* increase with the duration of the time horizon *H*. For example, for the 100-year horizon, these values are about -30 to +40% for methane (Reisinger et al., 2011).

Time horizon *H*, years	Methane CH_4		Carbon dioxide CO_2
	AGWP	*GWP*	*AGWP*
0	0	0	$1{,}096 \cdot 10^{-5}$
10	$2{,}510 \cdot 10^{-3}$	68,67	$3{,}656 \cdot 10^{-5}$
20	$3{,}601 \cdot 10^{-3}$	54,90	$6{,}560 \cdot 10^{-5}$
50	$4{,}371 \cdot 10^{-3}$	28,21	$1{,}549 \cdot 10^{-4}$
100	$4{,}439 \cdot 10^{-3}$	14,51	$3{,}059 \cdot 10^{-4}$

Table 3. Results of the calculation of methane and carbon dioxide emissions from the Nord Stream 1 and Nord Stream 2 pipelines

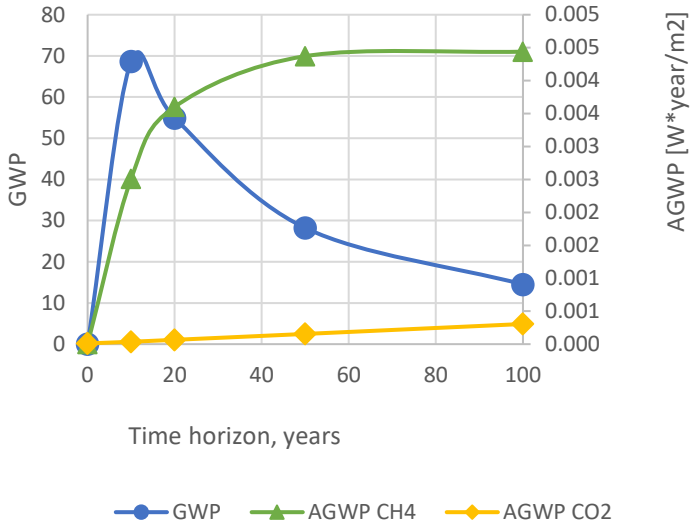

Figure 7. Model of the dependence of the global warming potential of the released methane and carbon dioxide on time

Based on the calculations of the *GWP* for methane and the composition of greenhouse gas emissions, the volume of methane emissions over the time horizon can be calculated by comparing them with the impact vehicles or cattle on temperature levels:

- in 10 years there will be an excess in the hydrocarbon cycle equivalent to 5.4936 megatons of CO_{2E} including the volume of methane emissions, which is comparable to carbon dioxide emissions of 1,672 million cars per year or carbon dioxide emissions from 2,3155 million head of cattle per year (Golubeva & Magaril, 2016; Vtorii & Vtorii, 2022);
- in 20 years, the excess compared to the natural level will drop to 4,3920 megatons of CO_{2E}, which is equivalent to the emissions of 1,337 million cars per year or 1,8512 million head of cattle per year;
- in 50 years, this value will be 2.2568 megatons of CO_{2E}, which is equivalent to the emissions of 0,687 million cars per year or 0,9512 million head of cattle per year;
- In 100 years it will be 1,1608 megatons of CO_{2E}, which is equivalent to the emissions of 0,353 million cars per year or 0,4893 million cattle per year.

Obviously, the peak impact of the gas leak will be observed within 10 years, after which the released gases will be absorbed and recycled by biota and chemical processes and ultimately removed from the cycle.

Other important measurable characteristics are the Global Temperature Change Potential (*GTP*), and the Absolute Global Temperature Change Potential (*AGTP*). *AGTP* is "the change in the average global temperature at a certain moment *H* in response to a one-time emission of a unit amount of a substance into the atmosphere at any moment *t,*" whereas the moment *t* may precede or coincide with the moment *H* for which the estimate is made.

For each greenhouse substance, as in the case of the global warming potential, we examine two characteristics - *AGTP* and the corresponding relative value, *GTP*, which is the ratio of the *AGTP* of the substance concerned and reference substance (reference matter) AGTP, which is usually carbon dioxide:

$$GTP = \frac{AGTP}{AGTP_r} \qquad (8)$$

Whereas *AGWP* and *GWP* estimate the effect of the release of a unit mass of a matter at the beginning of a time interval [0, *H*], based on the integral effect for the entire interval - the resulting radiation effect, *AGTP* and *GTP* estimate the effect on temperature only at the finite moment *H*.

As for *GWP*, the *GTP* metric is designed to obtain emission estimates for various greenhouse gases using the CO_2 equivalent. Like *GWP*, the corresponding weighting factors strongly depend on the time horizon used - the time between the moment of emission and the moment for which the effect is estimated (Lifshits et al., 2018).

Assuming linearity, *AGTP* can be conveniently used to estimate global temperature change $AGTP_i(H)$ over time for a given scenario of global $RF_i(t)$ of greenhouse gas emissions:

$$AGTP_i(H) = \int_0^H RF_i(t) R_T\,(H - t)dt \qquad (9)$$

Where i is the number of greenhouse gas, *H* is the present moment of time, *t* is the moment of emission

The global temperature change potential was calculated as follows:

$$R_T(t) = \sum_{j=1}^{M} \frac{c_j}{d_j} exp\left(-\frac{t}{d_j}\right) \qquad (10)$$

where R_T is the climate response to a single impact, which can be represented as a sum of exponents, where the c_j parameter denotes climate sensitivity components (K/W*m $^{-2}$) and d_j response time in years (Intergovernmental Panel on Climate Change 2013, 2014).

Using the above equations, *AGTP* over time horizon *H* for greenhouse gases other than CO_2 can be calculated as follows:

$$AGTP_i(H) = A_i \sum_{j=1}^{2} \frac{\tau c_j}{\tau - d_j} \left(exp\left(-\frac{H}{\tau}\right) - \exp\left(-\frac{H}{d_j}\right)\right) \qquad (11)$$

the *AGTP* for CO_2 is calculated as follows:

$$AGTP_{CO2}(H) = A_{CO2} \sum_{j=1}^{2} \{a_0 c_j \left(1 - exp\left(-\frac{H}{d_j}\right)\right) + \exp\left(-\frac{H}{d_j}\right)) +$$

$$\sum_{i=1}^{3} \{\frac{a_i \tau_i c_j}{\tau_i - d_j} \left(exp\left(-\frac{H}{\tau_i}\right) - \exp\left(-\frac{H}{d_j}\right)\right)\} \qquad (12)$$

Using the above formulas, the corresponding values for each of the indicators over the interval of the next hundred years (Intergovernmental Panel on Climate Change 2013, 2014) can be calculated (table 4, fig. 8) to obtain a model of global temperature change attributable to the observed emission of hydrocarbons and carbon dioxide from gas pipelines.

Both resulting models correlate with each other. It should be noted that in terms of the effect on global temperature, the peak value will be observed within the next 10 years (temperature increase by 0.0001 Kelvin).

Time horizon H, years	Methane CH_4		Carbon dioxide CO_2
	AGTP	GTP	AGTP
10	$1{,}042 \cdot 10^{-4}$	35,41	$2{,}942 \cdot 10^{-6}$
20	$7{,}869 \cdot 10^{-5}$	20,81	$3{,}781 \cdot 10^{-6}$
50	$1{,}421 \cdot 10^{-5}$	3,611	$3{,}935 \cdot 10^{-6}$
100	$3{,}934 \cdot 10^{-6}$	1,086	$3{,}623 \cdot 10^{-6}$

Table 4. Results of calculations of the global temperature change potential of methane and carbon dioxide emissions from the Nord Stream 1 and Nord Stream 2 pipelines

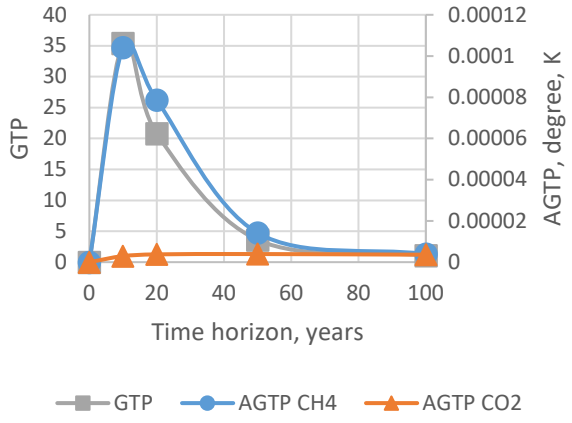

Figure 8. Model of the global temperature change potential of methane and carbon dioxide emitted as a result of the accident

Next, due to the integration of methane and carbon dioxide into natural biological and chemical processes, this value will decline, becoming nearly undetectable in 50 years.

5. CONCLUSION

The following preliminary facts have been established as a result of the study. The volume of leaks from each of the accident points was calculated, gas emission models were generated for the first time, the scope of failure of the underwater gas pipeline sections was estimated. In addition, the total volume of gas leakage from the Nord Stream system was determined to be approximately 0.08 megatons, helping us understand the general scale of the disaster.

The preliminary impact on the area where the leak occurred has been determined. Due to the fact that the water area in which the accident occurred belongs to the benthic "desert" zone, the impact of released gas on benthic organisms was minimal. The impact on phyto- and zooplankton was more significant. Some biota in the area of direct gas release and its mixing with water died. Large animals, the representatives of ichthyofauna and mammals left the accident area. The population density of marine mammals in this water area is low, and ichthyofauna feels oxygenation changes (due to the displacement of oxygen from the aquatic environment by methane) and leaves the water area if they are significant.

Along with the local impact of the released natural gas, its impact on temperature levels and the process of global warming (due to the integration of additional amounts of methane and carbon dioxide into the carbon cycle) was also assessed. The results suggest that the greatest effect of gas emissions would probably be observed within the next 10 years, with maximum *GWP* reference value for methane being 68.67CO_{2E}, which is equivalent to carbon dioxide emissions of 1,672 million cars per year or carbon dioxide emissions of 2,3155 million head of cattle per year, taking into account the volume of methane emission. Global temperature change potential calculations show that the peak value of temperature increase by 0.0001 Kelvin will also be observed within 10 years.

The described effects are reversible, because most of the methane that was released into the ecosystem will be removed within the next 20 years. The effects of the gas leakage on the ecosystem will disappear within 50 years. These results show the quantitative estimation for one of the greatest recent energy sector disasters. The data obtained fully cover the general technical and environmental consequences of the event, both at local and global levels. The impact on biota was modeled and consequences assessed. The obtained computational and analytical technical data and environmental forecast models are expected to be confirmed by future observations and studies conducted by the scientific community.

DECLARATION OF COMPETING INTEREST

The authors declare that they have no known financial or non-financial competing interests in any material discussed in this paper.

REFERENCES

Bezrodny, A. A., Yunushev, R. R., and Korolyonok, A. M., 2020. System analysis and efficient structure formation for gas station nets. Science Technologies Oil And Oil Products Pipeline Transportation, 10(1), 96–105. Available at: https://doi.org/10.28999/2541-9595-2020-10-1-96-105

Chen, X., and Zhou, T., 2023. Negligible warming caused by Nord Stream methane leaks, Advances in Atmospheric Sciences, 40, 549-552. Available at: https://doi.org/10.1007/s00376-022-2305-x

Dutz J., Kremp A. and Zettler M.L., 2022. Biological assessment of the Baltic Sea 2020. Marine Science Reports. 120, 82. Available at: http://doi.org/10.12754/msr-2022-0120

Environment and Energy: The Baltic Sea Gas Pipeline, 2013. Contemporary Environmentalism in the Baltic States, 163–186. Available at: https://doi.org/10.4324/9781315868172-13

Gillett, N.P. and Matthews, H.D., 2010. Accounting For Carbon Cycle Feedbacks in a Comparison of the Global Warming Effects of Greenhouse Gases, Environmental Research Letters, 5, 034011. Available at: https://doi.org/10.1088/1748-9326/5/3/034011

Gogina, M. et al., 2016. The Baltic Sea scale inventory of benthic faunal communities. ICES Journal of Marine Science, 73(4), 1196-1213. Available at: https://doi.org/10.1093/icesjms/fsv265

Golubeva, A. S., and Magaril, E. R., 2016. Economic Stimulation to Reduce Vehicle CO2 Emissions. Bulletin of Ural Federal University. Series Economics and Management, 15(3), 359–379. Available at: https://doi.org/10.15826/vestnik.2016.15.3.19

Gusev, A. and Rudinskaya, L., 2007. Macrozoobenthos along transect proposed line of the North European Gas Pipeline in the Baltic Sea in October 2005. VIII International Environmental Forum “Baltic Sea Day” (21-23 of March 2007, St. Petersburg). St. Petersburg, 270-271.

Haynes, M., and Daetwyler, N., 2012. Nord Stream: Ensuring Compliance with International HSE Standards and Managing Contractor HSE Performance. All Days. Available at: https://doi.org/10.2118/157221-ms

HELCOM, 2013. Red List of Baltic Sea species in danger of becoming extinct. Baltic Sea Environmental Proceedings, 140, 106.

Hersh S., 2023. How America took out the Nord Stream pipeline, 8.

Hinrichsen, H.-H. et al., 2007. Spatial and temporal heterogeneity of the cod spawning environment in the Bornholm Basin, Baltic Sea. Marine Ecology Progress Series. 345, 245-254. Available at: http://doi.org/10.3354/meps06989

ICES, 2021. Baltic Fisheries Assessment Working Group (WGBFAS). ICES Scientific Reports, 3, 717. Available at: https://doi.org/10.17895/ices.pub.8187

Intergovernmental Panel on Climate Change (IPCC), 2014. Technical Summary. In Climate Change 2013 – The Physical Science Basis: Working Group I Contribution to the Fifth Assessment Report of the Intergovernmental Panel on Climate Change (pp. 31-116). Cambridge: Cambridge University Press. Available at: https://doi.org/10.1017/CBO9781107415324.005

Jin, H., Zhang, L., Liang, W. and Ding, Q., 2014. Integrated leakage detection and localization model for gas pipelines based on the acoustic wave method, Journal of Loss Prevention in the Process Industries, 27, 74-88. Available at: https://doi.org/10.1016/j.jlp.2013.11.006

Karaseva, E.M., Zezera, A.S. and Ivanovich, V.M., 2012. Changes in the species composition and ichthyoplankton abundance along transects in the Baltic Sea. Oceanology, 52(4), 478–487. Available at: https://doi.org/10.1134/S0001437012040030

Karlson, K., Rosenberg, R. and Bonsdorff, E., 2002. Temporal and spatial large-scale effects of eutrophication and oxygen deficiency on benthic fauna in Scandinavian and Baltic waters – a review. Oceanography and Marine Biology: an Annual Review, 40, 427-489. Available at: https://doi.org/10.1201/9780203180594.ch8

Kiciński R., 2023. Estimating the Size of a Crater after an Underwater Explosion, Advances in Science and Technology, 17(5), 187-194. Available at: https://doi.org/10.12913/22998624/171503

Kuliński, K. et al., 2022. Biogeochemical functioning of the Baltic Sea. Earth System Dynamics, 13. 633-685. Available at: https://doi.org/10.5194/esd-13-633-2022

Leighton, T. G., and White, P. R., 2012. Quantification of undersea gas leaks from carbon capture and storage facilities, from pipelines and from methane seeps, by their acoustic emissions. Proceedings of the royal society A: mathematical, physical and engineering sciences, 468(2138), 485-510. Available at: https://doi.org/10.1098/rspa.2011.0221

Li, X., Wang, J. and Chen, G., 2022. A machine learning methodology for probabilistic risk assessment of process operations: A case of subsea gas pipeline leak accidents. Process Safety and Environmental Protection, 165, 959-968. Available at: https://doi.org/10.1016/j.psep.2022.04.029

Lifshits, S. Kh. et al., 2018. The Role of Methane and Methane Hydrates in the Evolution of Global Climate. American Journal of Climate Change, 07(02), 236–252. Available at: https://doi.org/10.4236/ajcc.2018.72016

Lu H., Xu, Z.D. et al., 2023. An inventory of greenhouse gas emissions due to natural gas pipeline incidents in the United States and Canada from 1980s to 2021, Scientific Data, 10(1), 282.

Lurie M. V., Musailov I. T. and Lysenko N. O., 2020. The Effective Method of Calculating Gas Leaks through Holes in the Walls of Gas Pipelines and High-Pressure Vessels, Territorija “NEFTEGAS”[Oil and Gas Territory], 3-4, 110-116.

Lurie, M. V., 2008. Fundamentals of mathematical modeling of one-dimensional flows of fluid and gas in pipelines. Modeling of Oil Product and Gas Pipeline Transportation, Wiley-VCH Verlag GmbH & Co. KGaA, Weinheim, Germany. Available at: https://doi.org/10.1002/9783527626199

Lurie, M. V., 2009. Modeling of Oil Product and Gas Pipeline Transportation / M. V. Lurie. – Weinheim: Wiley - VCH Verlag GmbH & CO. KGaA. Available at: https://doi.org/10.1002/9783527626199

McKeever, J. et al., 2019. Detection and Imaging of Methane Emissions Plumes from Oil and Gas Facilities with GHGSat-D. In AGU Fall Meeting Abstracts, pp. GC51M-0962. Available at: https://doi.org/10.5194/egusphere-egu2020-11184

Nikitina, L., 2014. Nord Stream and South Stream as innovative projects, their impact on the energy sector environment and policies of the European Union. Rocznik Integracji Europejskiej, (8), 377-388. Available at: https://doi.org/10.14746/rie.2014.8.26

Paka, V.T. and Nabatov V.N., 2022. Chemical weapons in the Baltic Sea: potential threats to the environment and public health; completed and upcoming tasks on the way to solving the problem. Journal of oceanological research. 50(2), 139–162. Available at: https://doi.org/10.29006/1564-2291.JOR-2022.50(1).7

Polunina, J.J., Krechik, V.A. and Paka, V.T., 2021. Spatial variability of zooplankton and hydrological indicators of the waters of the Southern and Central Baltic Sea in late summer of 2016. Oceanology, 61(6), 954-963. Available at: https://doi.org/10.1134/S0001437021060114

Pulch, R., and Günther, M., 2002. A method of characteristics for solving multirate partial differential equations in radio frequency application. Applied numerical mathematics, 42(1-3), 397-409. Available at: https://doi.org/10.1016/s0168-9274(01)00163-5

Reisinger, A., Meinshausen, M., and Manning, M., 2011. Future changes in global warming potentials under representative concentration pathways. Environmental Research Letters, 6(2), 024020. Available at: https://doi.org/10.1088/1748-9326/6/2/024020

Rolff, C., Walve, J. and Elmgren, R., 2022. How oxygen deficiency in the Baltic Sea proper has spread and worsened: the role of ammonium and hydrogen sulphide. AMBIO, 51(11), 2308-2324. Available at: https://doi.org/10.1007/s13280-022-01738-8

Sanderson H. et al., 2023. Environmental impact of sabotage of the Nord Stream pipelines, Research Square preprint deposition service. Available at: https://doi.org/10.21203/rs.3.rs-2564820/v1

Schulz, J. et al., 2012. Spatial and temporal habitat partitioning by zooplankton in the Bornholm Basin (central Baltic Sea). Progress in Oceanography, 107, 3-30. Available at: http://dx.doi.org/10.1016/j.pocean.2012.07.002

Shcherban, P.S. and Mazur, E.V., 2023. Preliminary assessment of the technical consequences of the incidents on the Nord stream 1 and 2 gas pipelines. Possible ways of solving the problems, International Journal for Quality Research, 17(2), 589–602. Available at: https://doi.org/10.24874/IJQR17.02-18

Stigebrandt, A. et al., 2015. Consequences of artificial deepwater ventilation in the Bornholm Basin for oxygen conditions, cod reproduction and benthic biomass – a model study, Ocean Science, 11(1), 93–110. Available at: https://doi.org/10.5194/os-11-93-2015

Strassmann, K., and Joos, F., 2017. The Bern Simple Climate Model (BernSCM) v1.0: an extensible and fully documented open source reimplementation of the Bern reduced form model for global carbon cycle-climate simulations. Geoscientific Model Development. Available at: https://doi.org/10.5194/gmd-2017-233

Tichý, L., and Dubský, Z., 2020. Russian energy discourse on the V4 countries. Energy Policy, 137, 111128. Available at: https://doi.org/10.1016/j.enpol.2019.111128

Vtorii, V.F. and Vtorii, S.V., 2022. Sources of carbon dioxide emissions on cattle dairy farms, Agrarian science of Euro-North-East, 23, 4. Available at: https://doi.org/10.30766/2072-9081.2022.23.4.572-579

Wasmund N. et al., 2019. Biological assessment of the Baltic Sea 2018. Marine Science Reports, 112, 99. Available at: http://doi.org/10.12754/msr-2019-0112

Yin R. and Zhong K., 2023. Nord stream explosions and the geopolitical game behind it, Law and power (Zakon i vlast), 1, 3-7.

Zavyalov, A.P. et al., 2023. On methods of ensuring energy efficiency of gas transportation under current conditions. Proceedings of Gubkin Russian State University of Oil and Gas, 1, 145–152. Available at: https://doi.org/10.33285/2073-9028-2023-1(310)-145-152

Zenkevich, L.A., 1963. Biology of the seas of the U.S.S.R. Available at: https://doi.org/10.5962/bhl.title.6447

Zettler M.L., Kremp A. and Dutz J., 2020. Biological assessment of the Baltic Sea 2019. Marine Science Reports, 115, 88. Available at: http://doi.org/10.12754/msr-2020-0115